

# Composite System Based on Chitosan and Room-Temperature Ionic Liquid: Direct Electrochemistry and Electrocatalysis of Hemoglobin

Xianbo Lu,<sup>†,‡</sup> Jianqiang Hu,<sup>†</sup> Xin Yao,<sup>†</sup> Zhouping Wang,<sup>†</sup> and Jinghong Li<sup>\*,†</sup>

Department of Chemistry, Key Lab. of Bioorganic Phosphorus Chemistry & Chemical Biology, Tsinghua University, Beijing 100084, China, and Department of Chemistry, University of Science and Technology of China, Hefei 230026, China

Received December 7, 2005; Revised Manuscript Received January 12, 2006

A novel polymer/room-temperature ionic liquid (RTIL) composite material based on chitosan (Chi) and 1-butyl-3-methyl-imidazolium tetrafluoroborate (BMIM·BF<sub>4</sub>) was explored. The composite system can be readily used as an immobilization matrix to entrap proteins and enzymes. Hemoglobin (Hb) was chosen as a model protein to investigate the composite system. A pair of well-defined quasireversible redox peaks of hemoglobin were obtained at the Chi–BMIM·BF<sub>4</sub>–Hb composite-film-modified glassy carbon (GC) electrode by direct electron transfer between the protein and the GC electrode. Dramatically enhanced biocatalytic activity was exemplified at the Chi–BMIM·BF<sub>4</sub>–Hb/GC electrode by the reduction of oxygen and trichloroacetic acid. Thermogravimetric analysis (TGA) suggests that the Chi–BMIM·BF<sub>4</sub>–Hb composite has higher thermal stability than Chi–Hb itself. The Chi–BMIM·BF<sub>4</sub>–Hb film was also characterized by UV–visible spectra, indicating excellent stability in solution and good biocompatibility for protein. The unique composite material based on polymer and ionic liquid can find wide potential applications in direct electrochemistry, biosensors, and biocatalysis.

## Introduction

Biocompatible materials have long been attracting increased attention worldwide because of their desirable properties and potential applications in biomedical,<sup>1</sup> biosensor,<sup>2</sup> biocatalysis,<sup>3</sup> bioelectronics,<sup>4</sup> and so on. As environmentally benign materials, they are nontoxic and biocompatible for bioactive proteins and enzymes, and even biodegradable. Biocompatible materials, which are generally composed of natural biomolecules,<sup>5</sup> biopolymers,<sup>6</sup> hydrogels,<sup>7</sup> bioceramics,<sup>8,9</sup> and nanomaterials,<sup>4,10</sup> can provide a favorable microenvironment for redox proteins and enzymes to realize direct electrochemistry and fabricate excellent biosensors. It is well-known that studies of direct electron transfer between redox-active proteins and electrodes are of great significance, which can provide a good model for understanding complex electron-transfer mechanisms in biological systems.<sup>11–15</sup> Direct electrochemistry of redox proteins can also establish a foundation for fabricating the third-generation biosensors,<sup>16,17</sup> biofuel cells,<sup>18,19</sup> biomedical devices,<sup>20</sup> enzymatic reactors,<sup>21</sup> etc.

Entrapment or encapsulation of an enzyme or protein within a biocompatible material by using simple procedures, especially physical entrapment of biomolecules without the need of complicated covalently attachment, is certainly desirable. A new composite system based on cellulose and ionic liquid has been reported by Rogers and co-workers.<sup>22,23</sup> They developed a new method for introducing active laccase into underivatized cellulosic matrixes through a cellulose-in-ionic-liquid dissolution and regeneration process. Biomolecules could be physically entrapped within the biocompatible cellulose matrix and demonstrate sustained activity, which may find applications in reactive and biocatalytic systems. The combination of RTIL and

polymer can create unique materials that might open up new opportunities for studies of direct electrochemistry, biosensors, biocatalysis,<sup>22</sup> and solid-state electrochemical devices.<sup>24</sup> However, our literature search revealed that no work has been reported on studies of direct electrochemistry and biosensors using a polymer/ionic liquid composite system.

Room-temperature ionic liquids (RTILs) are compounds consisting entirely of ions that exist in the liquid state around room temperature.<sup>25–29</sup> As novel attractive solvents, they possess unique properties such as negligible vapor pressure, wide potential windows, high thermal stability and high viscosity, and good conductivity and solubility.<sup>30</sup> In recent years, researchers have started to explore RTILs, especially 1-butyl-3-methyl-imidazolium tetrafluoroborate (BMIM·BF<sub>4</sub>) and 1-butyl-3-methyl-imidazolium hexafluorophosphate, as alternative media for biocatalysis.<sup>31,32</sup> Several groups<sup>33,34</sup> have reported increased thermal stability and activity of enzymes in the phosphate buffer solution containing BMIM·BF<sub>4</sub> as compared with aqueous buffer solution alone or conventional organic solvents. Another interesting application is to incorporate ionic liquids into conventional matrixes such as cellulose,<sup>22</sup> carbon materials,<sup>13,35</sup> and sol–gel-based silica matrixes.<sup>36</sup> Our group has obtained dramatically enhanced activity and excellent stability of horseradish peroxidase immobilized within a BMIM·BF<sub>4</sub> based sol–gel silica matrix.<sup>36</sup> However, the combinations of RTILs with these conventional matrixes are either a complicated and time-consuming process or lack good biocompatibility, which limit their wide applications.

Chitosan is a linear hydrophilic polysaccharide composed of  $\beta(1 \rightarrow 4)$  linked glucosamine units together with some proportion of *N*-acetylglucosamine units. It is an attractive biocompatible, biodegradable, and nontoxic natural biopolymer that exhibits excellent film-forming ability.<sup>6</sup> Because of its desirable properties, chitosan has been widely used as an immobilization matrix for biosensors and biocatalysis.<sup>37–40</sup> Considering its relatively poor conductivity, chitosan was usually combined with

\* Corresponding author. E-mail address: jhli@mails.tsinghua.edu.cn. Telephone: +86 10 6279 5290. Fax: +86 10 6279 5290.

<sup>†</sup> Department of Chemistry, Tsinghua University.

<sup>‡</sup> Department of Chemistry, University of Science and Technology of China.

carbon nanotubes,<sup>41</sup> redox mediators,<sup>42,43</sup> and metal nanoparticles<sup>44</sup> for electrochemical biosensing platforms.

In the present work, we explore a composite system based on chitosan and BMIM·BF<sub>4</sub>. BMIM·BF<sub>4</sub> (i.e., BMIM<sup>+</sup>BF<sub>4</sub><sup>-</sup>) is considered an excellent media for biocatalysis.<sup>31–34</sup> As a hydrophilic RTIL, BMIM·BF<sub>4</sub> can mix well with chitosan aqueous solution. The homogeneous solution of chitosan and BMIM·BF<sub>4</sub> can be readily made into different shapes (such as film, thread, and beads) after it is dried. BMIM·BF<sub>4</sub> (0.17 S/m at 25 °C) entrapped in the three-dimensional chitosan network can serve as an ionic conductor due to its good intrinsic conductivity. The composite system can be readily used as an immobilization matrix to entrap proteins and enzymes. We chose hemoglobin as a model protein to investigate the composite system. The composite system can provide a favorable microenvironment for the protein to retain its good bioactivity. Meanwhile, it can also provide a powerful platform for the protein to realize direct electron transfer with the underlying GC electrode. A Chi–BMIM·BF<sub>4</sub>–Hb composite film electrode was prepared by a very simple and general approach. Direct electrochemistry and electrocatalysis of hemoglobin were demonstrated at the Chi–BMIM·BF<sub>4</sub>–Hb composite-film-modified glassy carbon electrode. A pair of well-defined quasireversible redox peaks were obtained. Dramatically enhanced bioelectrocatalytic activity toward oxygen and trichloroacetic acid was also discussed.

## Experimental Section

**Materials and Solutions.** Chitosan (from crab shells, minimum 85% deacetylated) was purchased from Sigma. Hemoglobin (from bovine blood) was purchased from Beijing Century Forlin-Biotechnology Co., Ltd. BMIM·BF<sub>4</sub> (>98%, from Solvent Innovation, Germany) was purified according to ref 45. Trichloroacetic acid (TCA), NaH<sub>2</sub>PO<sub>4</sub>·2H<sub>2</sub>O, Na<sub>2</sub>HPO<sub>4</sub>·12H<sub>2</sub>O, HCl, and NaOH were purchased from Beijing Yili Chemical Reagent Corporation. Glycine was from Shanghai Chemical Reagent Corporation. All solutions were prepared by using Milli-Q purified water (>18.0 MQ) sterilized at high temperature.

The solution of 9.6 mg/mL hemoglobin was prepared by dissolving 96 mg hemoglobin in 10 mL of 50 mM pH 7.0 phosphate buffer solution (PBS). Chitosan (pK<sub>a</sub> = 6.3) can dissolve slowly in acidic aqueous solutions and form a viscous transparent solution. The 8 mg/mL chitosan aqueous solution (pH 5.0) was prepared mainly according to the previously reported procedure.<sup>41</sup> Briefly, chitosan was dissolved in 0.05 M HCl aqueous solution, and the pH of the chitosan solution was adjusted to 5.0 by using a 1.0 M NaOH solution. Then the chitosan solution was filtered using a 0.45- $\mu$ m cellulose syringe filter film (Automatic Science Instrument Co., Ltd., China). All solutions were stored in a refrigerator at 4 °C when not in use.

**Preparation of Film Electrode.** Prior to use, a 3-mm-diameter GC electrode was polished on a polishing cloth with alumina of successively smaller particles (1.0 and 0.05  $\mu$ m diameter). Then the electrode was cleaned by ultrasonication in deionized water, acetone, and ethanol, respectively. To obtain good cyclic voltammetric responses of the Hb–Chi–BMIM·BF<sub>4</sub>/GC electrode, the concentrations and the mass ratios of hemoglobin, chitosan, and BMIM·BF<sub>4</sub> were optimized in control experiments. Typically, a homogeneous solution (solution III) containing 1.2 mg/mL chitosan, 2.4 mg/mL hemoglobin, and 5% (V<sub>IL</sub>/V<sub>Total</sub>) BMIM·BF<sub>4</sub> was prepared by adding an appropriate volume of chitosan solution, hemoglobin solution, and pure BMIM·BF<sub>4</sub> into 50 mM pH 7.0 PBS. Then 6  $\mu$ L of solution III was cast onto the electrode surface by using a 10- $\mu$ L syringe to prepare a Hb–Chi–BMIM·BF<sub>4</sub>/GC electrode. A beaker was covered over the electrode so that water can evaporate slowly in air and a uniform film can be formed. The dried Chi–BMIM·BF<sub>4</sub>–Hb/GC electrode was stored at 4 °C in a refrigerator when not in use.

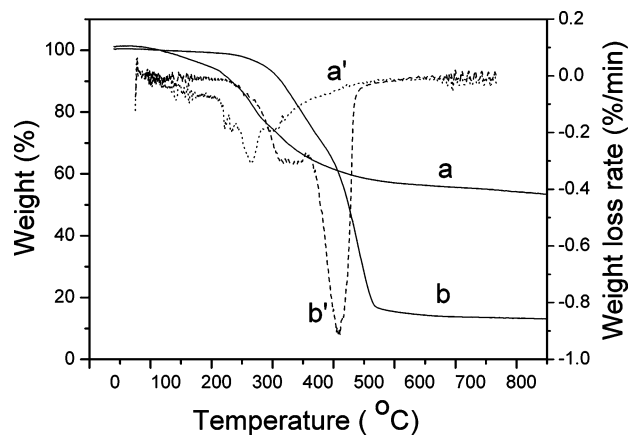


**Figure 1.** TGA (curve a and b) and DTG (dashed curve a' and b') curves of Chi–Hb (curve a and a') and Chi–Hb–BMIM·BF<sub>4</sub> (curve b and b'). Measurements were performed by heating the samples from 40 to 750 °C at a heating rate of 10 °C/min under flowing Argon atmosphere.

For comparison with the Chi–BMIM·BF<sub>4</sub>–Hb/GC electrode, Hb/GC and Hb–Chi/GC electrodes were prepared with the same procedures as described above. A solution (solution I, pH 7.0) containing 2.4 mg/mL hemoglobin was used to prepare the Hb/GC electrode, and another solution (solution II, pH 7.0) containing 2.4 mg/mL hemoglobin and 1.2 mg/mL chitosan was used to prepare the Hb–Chi/GC electrode. Before electrochemical measurements, all the as-prepared film electrodes were immersed in buffer solution for 30 min to remove the residual composites (physically absorbed BMIM·BF<sub>4</sub> or Hb).

**Electrochemical Measurements.** Experiments were performed at room temperature by using a CHI 830 workstation (CH Instruments, Inc.). The electrochemical measurements were based on a conventional three-electrode system with the as-prepared film electrode as the working electrode, a platinum wire as the auxiliary electrode, and an Ag/AgCl (saturated KCl) electrode as the reference electrode. A 50 mM phosphate buffer solution or 50 mM glycine–hydrochloric acid (GHA, pH 3.0) buffer solution were used as the electrolytes in all experiments. The buffer solutions were purged with highly purified nitrogen for at least 30 min by continuously bubbling nitrogen before measurements, and a nitrogen atmosphere environment was kept in electrochemical measurements.

**Thermogravimetric and Spectroscopic Analysis.** The thermogravimetric analysis (TGA) was performed with a STA 409C thermal analyzer (NETZSCH, Germany). The samples of Hb–Chi and Hb–Chi–BMIM·BF<sub>4</sub> were prepared by evaporating water of solutions of Hb–Chi and Hb–Chi–BMIM·BF<sub>4</sub> in a vacuum desiccator, respectively. Measurements were conducted by heating the as-prepared samples from 40 to 750 °C at a heating rate of 10 °C/min under flowing argon atmosphere. The mass ratio of Hb to Chi in the Hb–Chi sample was 4:3, which was the same as in the Hb–Chi–BMIM·BF<sub>4</sub> sample.

UV–vis measurements were carried out by using a 2100S spectrophotometer (Shimadzu, Japan). Sample films for measurements were prepared by casting Hb solution (solution I) or Hb–Chi–BMIM·BF<sub>4</sub> solution (solution III) onto quartz glass slides and drying them in air. The obtained dry Hb/glass and Hb–Chi–BMIM·BF<sub>4</sub>/glass films were detected.

## Results and Discussion

**Characterization by TGA and UV–Vis Absorption Spectra.** Figure 1 shows the comparative thermogravimetric analysis curves (curve a and b) and differential thermogravimetric (DTG) curves (curve a' and b') of Hb–Chi (curve a and a') and Hb–Chi–BMIM·BF<sub>4</sub> (curve b and b'). The onset temperatures of weight loss process for Hb–Chi and Hb–Chi–BMIM·BF<sub>4</sub> samples were about 160 °C and 240 °C, respectively. As shown

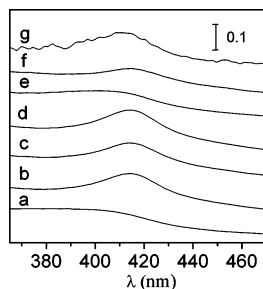


**Figure 2.** UV-vis absorption spectra of dry Hb film (g), dry Hb-Chi-BMIM·BF<sub>4</sub> film (f), and the Hb-Chi-BMIM·BF<sub>4</sub> film immersed in different pH buffers: (a) pH 3.0, (b) pH 5.0, (c) pH 7.0, (d) pH 9.0, (e) pH 11.0. To demonstrate clearly, the curves were shifted along the y-axis.

in Figure 1, the thermal decomposition of Hb-Chi took place mainly at 200–400 °C with a narrow peak at 260 °C (maximum weight loss rate). Zhang et al.<sup>41</sup> reported that the thermal decomposition of Chi at 200–400 °C could be ascribed to the depolymerization and decomposition of glucosamine units of Chi. Different from that of Hb-Chi, the DTG curve of Hb-Chi-BMIM·BF<sub>4</sub> has a plateau at 320–380 °C and a well-defined narrow peak at 440 °C between 380 and 480 °C. The narrow peak corresponds to the decomposition of BMIM·BF<sub>4</sub>, and the mass loss before reaching 380 °C is mainly attributed to the decomposition of Hb and Chi. The thermal stability of Hb-Chi-BMIM·BF<sub>4</sub> is higher than that of Hb-Chi itself, which should be ascribed to the interaction between Hb-Chi and BMIM·BF<sub>4</sub>. Similar results have been reported in other polymer/ionic liquid systems.<sup>24, 46</sup>

UV-vis absorption spectroscopic analysis is an effective means to probe into the secondary structure of proteins. The position of a Soret absorption band of heme (Fe) can provide information about possible denaturing of heme protein.<sup>37,47</sup> Figure 2 shows that the dry Hb (curve g) and Hb-Chi-BMIM·BF<sub>4</sub> (curve f) films have the same Soret absorption band at about 415 nm, indicating that the Hb entrapped in Hb-Chi-BMIM·BF<sub>4</sub> film has a similar secondary structure to the Hb in its dry film alone. Curves a–e of Figure 2 give UV-vis absorption spectra of Hb-Chi-BMIM·BF<sub>4</sub> film immersed in different pH buffer solutions, indicating that the Soret absorption band position of Hb in Hb-Chi-BMIM·BF<sub>4</sub> film depends on the pH of buffer solution. At pH 5, 7, and 9, the Soret absorption band position of Hb appeared at 415 nm, the same as that of dry Hb and Hb-Chi-BMIM·BF<sub>4</sub> film, as well as that of Hb solution at the same pH. This reveals that Hb retained its essential conformation in dry Hb-Chi-BMIM·BF<sub>4</sub> film and in the case that Hb-Chi-BMIM·BF<sub>4</sub> film was immersed in a solution of medium pH range (about pH 5–9). When the pH of solution decreased from 5 to lower or increased from 9 to higher, the Soret absorption band became broader. As shown in curve a and curve e in Figure 2, the Soret absorption bands disappeared at pH 3 and pH 11, suggesting conformational change of Hb in Hb-Chi-BMIM·BF<sub>4</sub> film at these acidic or alkaline pH environments. It should be noted that the conformational change of Hb in Hb-Chi-BMIM·BF<sub>4</sub> film under these conditions was temporary and reversible. When the Hb-Chi-BMIM·BF<sub>4</sub> film was placed in a medium pH range again, the disappeared Soret absorption band appeared at 415 nm again. All these results indicate that the system based on chitosan and BMIM·BF<sub>4</sub> does not denature Hb and has good biocompatibility for Hb.

To study the stability of Hb-Chi-BMIM·BF<sub>4</sub>/glass film by spectroscopy, we collected the UV-vis absorption spectra of

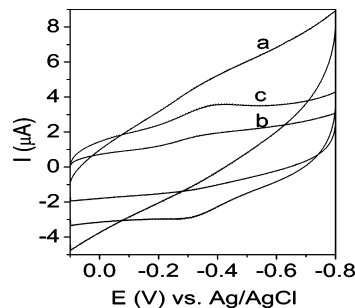


**Figure 3.** Cyclic voltammograms of Hb (equal mass amount Hb) at different modified electrodes in 50 mM pH 7.0 PBS: (a) Hb/GC, (b) Hb-Chi/GC, (c) Hb-Chi-BMIM·BF<sub>4</sub>/GC. Scan rate: 0.2 V/s.

dry Hb-Chi-BMIM·BF<sub>4</sub>/glass film immersed in pH 7.0 PBS for different times. There was no obvious change of absorption spectra after 24 h, suggesting the Hb-Chi-BMIM·BF<sub>4</sub> film was very stable in PBS. The negligible peak intensity shift (within 3% after 24 h) of the Soret absorption band after such a long time indicates that Hb in Hb-Chi-BMIM·BF<sub>4</sub> film almost entirely retained its native conformation. It further indicates that Hb in Hb-Chi-BMIM·BF<sub>4</sub> film would not diffuse into buffer solution. Both the good biocompatibility of the composite system and the strong interaction between Hb and Chi-BMIM·BF<sub>4</sub> contribute to the excellent stability of Hb-Chi-BMIM·BF<sub>4</sub> film.

**Electrochemical Properties.** Figure 3 shows typical cyclic voltammograms of Hb at different electrodes in 50 mM pH 7.0 PBS. A pair of well-defined redox peaks, which could be ascribed to the electron transfer between the hemoglobin and the underlying electrode, were observed at the Hb-Chi-BMIM·BF<sub>4</sub>/GC electrode (curve c in Figure 3). No obvious redox peak was observed at the Hb/GC (curve a in Figure 3) or Hb-Chi/GC electrodes (curve b in Figure 3), which is possibly due to the unfavorable orientation or denaturing of hemoglobin molecules on the bare GC electrode surface, or the poor conductivity of chitosan that hinders the direct electron transfer between hemoglobin and the GC electrode. Compared with the Hb/GC or Hb-Chi/GC electrodes, BMIM·BF<sub>4</sub> entrapped in the Hb-Chi-BMIM·BF<sub>4</sub>/GC electrode can provide a conducive microenvironment that facilitates the electron transfer between the hemoglobin and the GC electrode. According to  $Q = nFA\Gamma^*$  (where  $F = 96485$ ,  $Q$  represents the average reacted electric quantity,  $\Gamma^*$  is the electroactive hemoglobin amount,  $n$  and  $A$  stand for the number of electrons transferred and the area of the GC electrode, respectively), the amount of electroactive hemoglobin molecules at the Hb-Chi-BMIM·BF<sub>4</sub>/GC electrode was estimated to be  $6.31 \times 10^{-11}$  mol cm<sup>-2</sup> (assuming a one-electron-transfer reaction), which is almost 3 times higher than that reported.<sup>37</sup> The value obtained in our experiment is about 3.3 times higher than that of the theoretical monolayer coverage ( $1.89 \times 10^{-11}$  mol cm<sup>-2</sup>).<sup>48</sup> This shows that several layers of hemoglobin entrapped in the three-dimensional composite film participated in the electron-transfer process. The percentage of the electroactive Hb on the electrode surface was about 2.0%, which is always relative low because only those proteins in the inner layers of the film close to the electrode and with a suitable orientation can exchange electrons with the electrode surface.<sup>48</sup> The formal potential  $E^{\circ'}$  (estimated as  $(E_{p,a} + E_{p,c})/2$ , where  $E_{p,a}$  and  $E_{p,c}$  are the anodic and cathodic peak potentials, respectively) of hemoglobin was  $-0.34$  V vs Ag/AgCl, which was characteristic of the potential of heme (Fe<sup>III/II</sup>) redox couples and was consistent with the literature.<sup>14,17,37,48–50</sup> The peak separation  $\Delta E_p$  (defined as  $\Delta E_p = E_{p,a} - E_{p,c}$ ) was

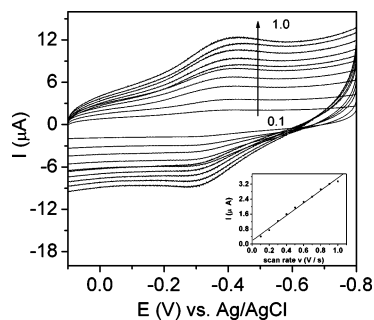


**Figure 4.** Cyclic voltammograms of Hb–Chi–BMIM·BF<sub>4</sub>/GC electrodes in pH 7.0 PBS with scan rates of 0.1–1.0 V/s. Inset: plot of the cathodic peak currents vs scan rates.

56 mV, and the ratio of  $I_{p,c}/I_{p,a}$  was approximately 1, which are all characteristics of a quasireversible redox process.

Figure 4 gives the typical cyclic voltammograms of the Hb–Chi–BMIM·BF<sub>4</sub>/GC electrode in pH 7 PBS with scan rates of 0.1–1.0 V/s. With the increase of the scan rate, the cathodic and anodic peak currents increased simultaneously. As shown in the inset of Figure 4, the cathodic peak currents ( $I_{p,c}$ ) are linear, with scan rates from 0.1 to 1.0 V/s. This reveals that the electron transfer of hemoglobin with the GC electrode is a surface-confined electrochemical process, which is similar to a surfactant- or clay-modified hemoglobin film electrode<sup>50,51</sup> and is different from the diffusion-controlled process of DDAB/Hb-modified graphic electrodes.<sup>52</sup>

The formal potential of hemoglobin showed strong dependence on the pH of buffer solution. The anodic and cathodic peak potentials shifted negatively with increasing pH. The formal potentials of hemoglobin had a linear dependence on pH with a slope of  $-40.5$  mV/pH (pH 3.0–11.0), indicating a proton-coupled electron-transfer process. The slope was smaller than the previous report,<sup>37</sup> in which the slope was  $-52.4$  mV/pH (pH 5.5–12.0). The difference probably resulted from the different microenvironments, especially the BMIM·BF<sub>4</sub> in Hb–Chi–BMIM·BF<sub>4</sub>/GC. As a Lewis acid base pair, BMIM·BF<sub>4</sub> possibly provided a more stable microenvironment for hemoglobin to be less influenced by the pH of buffer solution.

The stability of the Hb–Chi–BMIM·BF<sub>4</sub>/GC electrode in buffer solution was tested by comparing the reduction peak currents of hemoglobin with time intervals of 4 h. The Hb–Chi–BMIM·BF<sub>4</sub>/GC electrode was immersed in buffer solution all the time during the 4 h. We have proved by UV–vis measurements that Hb entrapped in Hb–Chi–BMIM·BF<sub>4</sub> composite film could not diffuse into buffer solution in 24 h. However, leaching of BMIM·BF<sub>4</sub> from the Hb–Chi–BMIM·BF<sub>4</sub>/GC electrode will also result in a decrease of redox peak currents of hemoglobin due to the decrease of conductivity of the composite film. Experimental results proved that the decrease of reduction peak currents was about 1.6%, indicating that BMIM·BF<sub>4</sub> entrapped in the Hb–Chi–BMIM·BF<sub>4</sub>/GC electrode could not diffuse into buffer solution. The slight change of cyclic voltammograms after 50 consecutive cyclic voltammetric scans also proved that the Hb–Chi–BMIM·BF<sub>4</sub>/GC composite film electrode was very stable. Although BMIM·BF<sub>4</sub> and hemoglobin are water soluble to some extent, the interactions between BMIM·BF<sub>4</sub>, hemoglobin, and chitosan are strong enough to prevent them from leaching into buffer solution. The interactions in the composite system based on chitosan, BMIM·BF<sub>4</sub>, and hemoglobin are complicated, containing electrostatic, hydrogen bond, charge–charge interaction,<sup>32</sup> van der Waals force, hydrophilic, and hydrophobic interactions.

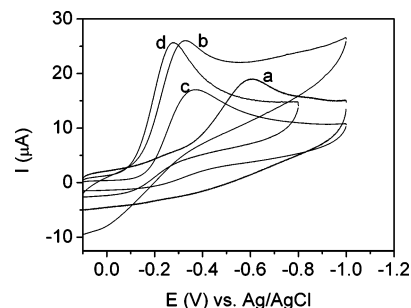
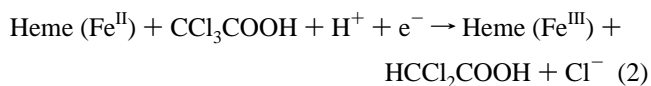


**Figure 5.** Electrochemical reduction of O<sub>2</sub> at different electrodes in pH 7.0 PBS without deoxy: (a) bare GC, (b) Hb/GC, (c) Hb–Chi/GC, (d) Hb–Chi–BMIM·BF<sub>4</sub>/GC. Scan rate: 0.1 V/s.

The good stability of the Hb–Chi–BMIM·BF<sub>4</sub>/GC electrode in buffer solution could be mainly ascribed to the good biocompatibility of the composite system and the strong interactions within the composite system.

**Electrocatalytic Properties.** As one kind of heme (Fe) protein, bioactive hemoglobin immobilized on an electrode surface usually has good electrocatalytic activity for oxygen, TCA, NO<sub>2</sub><sup>−</sup>, H<sub>2</sub>O<sub>2</sub>, etc.<sup>37</sup> Taking oxygen and TCA as examples, we studied the electrocatalytic properties of the Hb–Chi–BMIM·BF<sub>4</sub>/GC electrode. The comparison of electrocatalytic reduction toward O<sub>2</sub> at different electrodes is demonstrated in Figure 5. As shown, the electrocatalytic reduction potential of O<sub>2</sub> at the Hb–Chi–BMIM·BF<sub>4</sub>/GC electrode (curve d in Figure 5) was about  $-0.28$  V, which was more positive than that observed at the Hb/GC ( $-0.33$  V, curve b in Figure 5) and the Hb–Chi/GC electrode ( $-0.35$  V, curve c in Figure 5), indicating better bioelectrocatalytic ability of the Hb–Chi–BMIM·BF<sub>4</sub>/GC electrode than the Hb–Chi/GC and Hb/GC electrodes toward O<sub>2</sub>. Compared with direct electrochemical reduction of O<sub>2</sub> at the bare GC electrode (about  $-0.6$  V, curve a in Figure 5), the Hb–Chi–BMIM·BF<sub>4</sub>/GC electrode lowered the reduction overpotential of O<sub>2</sub> by at least 0.3 V. The experimental results indicate that hemoglobin retains its excellent bioactivity at the Hb–Chi–BMIM·BF<sub>4</sub>/GC electrode. It further indicates that, besides hemoglobin, BMIM·BF<sub>4</sub> entrapped in chitosan also contributes to the electrochemical reduction of O<sub>2</sub> at the Hb–Chi–BMIM·BF<sub>4</sub>/GC electrode. The good conductivity of BMIM·BF<sub>4</sub> facilitates the electron transfer in the three-dimensional Hb–Chi–BMIM·BF<sub>4</sub> film and thus results in better bioelectrocatalytic activity of the Hb–Chi–BMIM·BF<sub>4</sub>/GC than the Hb–Chi/GC electrode toward O<sub>2</sub>.

As is well-known, TCA is an important organohalide environmental pollutant. To detect the concentration of TCA in the environment is of great importance for controlling pollution. The electrocatalytic reduction of TCA by the Hb–Chi–BMIM·BF<sub>4</sub>/GC electrode in pH 3.0 GHA buffer solution is shown in Figure 6. When TCA was added to GHA buffer solution, a reduction peak was observed at about  $-0.288$  V, accompanying the decrease of the oxidation peak of hemoglobin. No electrochemical reduction peak was observed when the cyclic voltammetric scan was performed at bare the GC or the chitosan-modified GC electrode under the same conditions. The mechanism of bioelectrocatalytic reduction of TCA by hemoglobin might be schematically expressed as follows:<sup>12</sup>



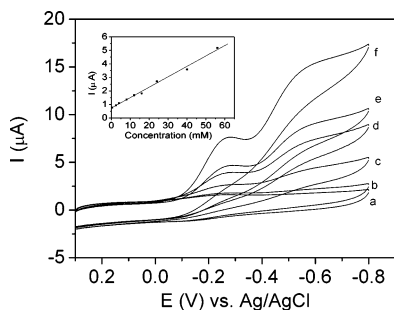


**Figure 6.** Electrocatalytic reduction of different TCA concentrations at the Hb–Chi–BMIM·BF<sub>4</sub>/GC electrode in 50 mM pH 3.0 GHA buffer solution with scan rate 0.1 V/s: (a) 0 mM TCA, (b) 0.4 mM, (c) 8.0 mM, (d) 24.0 mM, (e) 40.0 mM, (f) 56.0 mM. Inset: plot of the reduction peak currents vs concentrations of TCA.

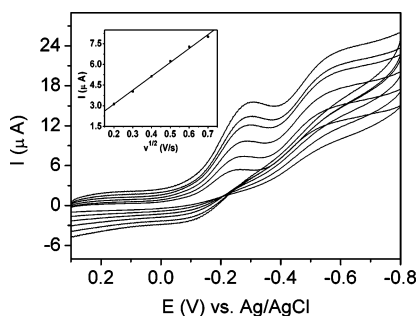
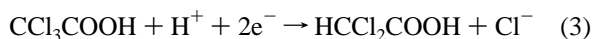


**Figure 7.** Cyclic voltammograms of the Hb–Chi–BMIM·BF<sub>4</sub>/GC electrode in the presence of 56 mM TCA with scan rates of 0.04, 0.09, 0.16, 0.25, 0.36, and 0.49 V/s, respectively. Inset: plot of the peak current vs the square root of the scan rate. Supporting electrolyte: 50 mM pH 3.0 GHA buffer solution under nitrogen.

The overall reaction would be:



The reduction peak currents increase linearly with concentrations of TCA from 0.4 to 56 mM, as shown in the inset of Figure 6. The linear regression equation is  $y = 0.077x + 0.738$ , where  $y$  and  $x$  stand for the peak current ( $\mu\text{A}$ ) and the concentration (mM) of TCA, respectively. The Hb–Chi–BMIM·BF<sub>4</sub>/GC electrode may be used to detect organohalide pollutants in the environment.

Figure 7 demonstrates the cyclic voltammograms of the Hb–Chi–BMIM·BF<sub>4</sub>/GC electrode in the presence of 56 mM TCA with different scan rates. It can be clearly seen from Figure 7 that, with increased scan rates, the catalytic peak currents increase and the peak potentials slightly shift toward negative. The relationship between the peak currents and the square roots of the scan rates is shown in the inset of Figure 7. The peak currents vary linearly with the square roots of scan rates from 0.04 to 0.49 V/s, and the catalytic efficiency (expressed as the ratio of reduction peak currents in the presence and absence of TCA) decreases with increasing scan rate, indicating a diffusion-controlled electrocatalytic process. Compared with the Hb–Chi–BMIM·BF<sub>4</sub>/GC electrode, there was no obvious peak observed at the Hb/GC or Hb–Chi/GC electrodes in the presence of 40 mM TCA (figures not shown). The dramatically enhanced bioelectrocatalytic activity of Hb at the Hb–Chi–BMIM·BF<sub>4</sub>/GC electrode should be ascribed to the BMIM·BF<sub>4</sub> entrapped in Hb–Chi–BMIM·BF<sub>4</sub> film. The BMIM·BF<sub>4</sub> entrapped in the Hb–Chi–BMIM·BF<sub>4</sub>/GC electrode is essential for direct electrochemistry and electrocatalysis of hemoglobin, which facilitates the electron transfer between the hemoglobin and the electrode. Both biocompatibility of chitosan and inherent

conductivity of BMIM·BF<sub>4</sub> enable the composite material to become an excellent biosensing platform for realizing direct electrochemistry and electrocatalysis of hemoglobin along with good stability.

## Conclusion

We explored a novel composite material based on chitosan and BMIM·BF<sub>4</sub>. The composite material can be readily used as an immobilization matrix to entrap proteins and enzymes. As an example, we chose redox-active hemoglobin as a model protein to investigate the composite system. A simple and general method was used to prepare the bioactive Hb–Chi–BMIM·BF<sub>4</sub>/GC composite film electrode. The obtained results revealed that direct electron transfer between redox proteins and the underlying electrode can be easily performed at the Hb–Chi–BMIM·BF<sub>4</sub>/GC composite film electrode and the composite film electrode had dramatically enhanced bioelectrocatalytic activity toward oxygen and trichloroacetic acid along with good stability in solution. The unique composite material can provide a good electrochemical sensing platform for redox proteins and enzymes, and thus it is expected to have widely potential applications in direct electrochemistry, biosensors, and biocatalysis.

**Acknowledgment.** This work was supported financially by the National Natural Science Foundation of China (no. 20125513, no. 20435010, no. 20575032), the Li Foundation Heritage Prize, United States, and the Foundation for the Author of National Excellent Doctoral Dissertation of PR China.

## References and Notes

- Ghosh, S. J. *Chem. Res., Synop.* **2004**, *4*, 241–246.
- Zhou, G. J.; Wang, G.; Xu, J. J.; Chen, H. Y. *Sens. Actuators, B* **2002**, *81*, 334–339.
- Cho, B. K.; Cho, H. J.; Yun, H.; Kim, B. G. *J. Mol. Catal. B: Enzym.* **2003**, *26*, 273–285.
- Katz, E.; Willner, I. *Angew. Chem., Int. Ed.* **2004**, *43*, 6042–6108.
- Paolucci-Jeanjean, D.; Belleville, M. P.; Rios, G. M. *Chem. Eng. Res. Des.* **2005**, *83*, 302–308.
- Peniche, C.; Argiuelles-Monal, W.; Peniche, H.; Acista, N. *Macromol. Biosci.* **2003**, *3*, 511–520.
- Iwasaki, Y.; Nakagawa, C.; Ohtomi, M.; Akiyoshi, K. *Biomacromolecules* **2004**, *5*, 1110–1115.
- Tian, D.; Dubois, P.; Grandfils, C.; Jerome, R.; Viville, P.; Lazzaroni, R.; Bredas, J. L.; Leprince, P. *Chem. Mater.* **1997**, *9*, 871–874.
- Silva, C. C.; Rocha, H. H. B.; Freire, F. N. A.; Santos, M. R. P.; Saboia, K. D. A.; Goes, J. C.; Sombra, A. S. B. *Mater. Chem. Phys.* **2005**, *92*, 260–268.
- Li, Z.; Wei, L.; Gao, M. Y.; Lei, H. *Adv. Mater.* **2005**, *17*, 1001–1005.
- Armstrong, F. A. *J. Chem. Soc., Dalton Trans.* **2002**, 661–671.
- Hu, N. F. *Pure Appl. Chem.* **2001**, *73*, 1979–1991.
- Zhao, Q.; Zhan, D. P.; Ma, H. Y.; Zhang, M. Q.; Zhao, Y. F.; Jing, P.; Zhu, Z. W.; Wan, X. H.; Shao, Y. H.; Zhuang, Q. K. *Front. Biosci.* **2005**, *10*, 326–334.
- Liu, H. Y.; Rusling, J. F.; Hu, N. F. *Langmuir* **2004**, *20*, 10700–10705.
- Rusling, J. F. *Acc. Chem. Res.* **1998**, *31*, 363–369.
- Jia, J. B.; Wang, B. Q.; Wu, A. G.; Cheng, G. J.; Li, Z.; Dong, S. J. *Anal. Chem.* **2002**, *74*, 2217–2223.
- Liu, S. Q.; Dai, Z. H.; Chen, H. Y.; Ju, H. X. *Biosens. Bioelectron.* **2004**, *19*, 963–969.
- Ramanavicius, A.; Kausaite, A.; Ramanaviciene, A. *Biosens. Bioelectron.* **2005**, *20*, 1962–1967.
- Barton, S. C.; Gallaway, J.; Atanassov, P. *Chem. Rev.* **2004**, *104*, 4867–4886.
- Palmisano, F.; Zamboni, P. G.; Centonze, D.; Quinto, M. *Anal. Chem.* **2002**, *74*, 5913–5918.
- Wong, T. S.; Schwaneberg, U. *Curr. Opin. Biotechnol.* **2003**, *14*, 590–596.

- (22) Turner, M. B.; Spear, S. K.; Holbrey, J. D.; Rogers, R. D. *Biomacromolecules* **2004**, *5*, 1379–1384.
- (23) Swatloski, R. P.; Spear, S. K.; Holbrey, J. D.; Rogers, R. D. *J. Am. Chem. Soc.* **2002**, *124*, 4974–4975.
- (24) Susan, M. A. B. H.; Kaneko, T.; Noda, A.; Watanabe, M. *J. Am. Chem. Soc.* **2005**, *127*, 4976–4983.
- (25) Moulthrop, J. S.; Swatloski, R. P.; Moyna, G.; Rogers, R. D. *Chem. Commun.* **2005**, 1557–1559.
- (26) Luo, H. M.; Dai S.; Bonnesen, P. V.; Buchanan, A. C.; Holbrey, J. D.; Bridges, N. J.; Rogers, R. D. *Anal. Chem.* **2004**, *76*, 3078–3083.
- (27) Li, J. H.; Shen, Y. F.; Zhang, Y. J.; Liu, Y. *Chem. Commun.* **2005**, 360–362.
- (28) Li, Z. Y.; Liu, H. T.; Liu, Y.; He, P.; Li, J. H. *J. Phys. Chem. B.* **2004**, *108*, 17512–17518.
- (29) Liu, Y.; Wang, M. J.; Li, Z. Y.; Liu, H. T.; He, P.; Li, J. H. *Langmuir* **2005**, *21*, 1618–1622.
- (30) Buzzeo, M. C.; Hardacre, C.; Compton, R. G. *Anal. Chem.* **2004**, *76*, 4583–4588.
- (31) Park, S.; Kazlauskas, R. *Curr. Opin. Biotechnol.* **2003**, *14*, 432–437.
- (32) Laszlo, J. A.; Compton, D. L. *J. Mol. Catal. B: Enzym.* **2002**, *18*, 109–120.
- (33) Machado, M. F.; Saraiva, J. M. *Biotechnol. Lett.* **2005**, *27*, 1233–1239.
- (34) Lou, W. Y.; Zong, M. H.; Wu, H. *Biocatal. Biotransform.* **2004**, *22*, 171–176.
- (35) Zhao, F.; Wu, X. E.; Wang, M. K.; Liu, Y.; Gao, L. X.; Dong, S. J. *Anal. Chem.* **2004**, *76*, 4960–4967.
- (36) Liu, Y.; Wang, M.; Li, J.; He, P.; Liu, H. T.; Li, J. H. *Chem. Commun.* **2005**, 1778–1780.
- (37) Huang, H.; Hu, N. F.; Zeng, Y. H.; Zhou, G. *Anal. Biochem.* **2002**, *308*, 141–151.
- (38) Bindhu, L. V.; Abraham, E. T. *J. Appl. Polym. Sci.* **2003**, *88*, 1456–1464.
- (39) Coche-Guerente, L.; Desbrieres, J.; Fatisson, J.; Labbe, P.; Rodriguez, M. C.; Rivas, G. *Electrochim. Acta* **2005**, *50*, 2865–2877.
- (40) Xu, J. J.; Luo, X. L.; Du, Y.; Chen, H. Y. *Electrochem. Commun.* **2004**, *6*, 1169–1173.
- (41) Zhang, M. G.; Smith, A.; Gorski, W. *Anal. Chem.* **2004**, *76*, 5045–5050.
- (42) Zhang, M.; Gorski, W. *J. Am. Chem. Soc.* **2005**, *127*, 2058–2059.
- (43) Luo, X. L.; Xu, J. J.; Wang, J. L.; Chen, H. Y. *Chem. Commun.* **2005**, 2169–2171.
- (44) Luo, X. L.; Xu, J. J.; Du, Y.; Chen, H. Y. *Anal. Biochem.* **2004**, *334*, 284–289.
- (45) Lin, L. G.; Wang, Y.; Yan, J. W.; Yuan, Y. Z.; Xiang, J.; Mao, B. W. *Electrochem. Commun.* **2003**, *5*, 995–999.
- (46) Snedden, P.; Cooper, A. I.; Scou, K.; Winterton, N. *Macromolecules* **2003**, *36*, 4549–4556.
- (47) Theorell, H.; Ehrenberg, A. *Acta Chem. Scand.* **1951**, *5*, 823–848.
- (48) Wang, S. F.; Chen, T.; Zhang, Z. L.; Shen, X. C.; Lu, Z. X.; Pang, D. W.; Wong, K. Y. *Langmuir* **2005**, *21*, 9260–9266.
- (49) Liu, H. Y.; Wang, L. W.; Hu, N. F. *Electrochim. Acta.* **2002**, *47*, 2515–2523.
- (50) Zhou, Y. L.; Hu, N. F.; Zeng, Y. H.; Rusling, J. F. *Langmuir* **2002**, *18*, 211–219.
- (51) Fan, C. H.; Suzuki I.; Chen, Q.; Li, G. X.; Anzai, J. *Anal. Lett.* **2000**, *33*, 2631–2644.
- (52) Mimica, D.; Zagal, J. H.; Bedioui, F. *J. Electroanal. Chem.* **2001**, *497*, 106–113.

BM050933T